

## ANALYSIS OF BEAM LOSSES AT PSR\*

R. J. Macek, D. H. Fitzgerald, R. L. Hutson, M. A. Plum, and H. A. Thiessen  
 Los Alamos National Laboratory  
 Mail Stop H848  
 Los Alamos, NM 87545 USA

Abstract

Beam losses and the resulting component activation at the Los Alamos Proton Storage Ring (PSR) have limited operating currents to about  $30 \mu\text{A}$  average at a repetition rate of 15 Hz. Loss rates were found to be approximately proportional to the circulating current and can be understood by a detailed accounting of emittance growth in the two step injection process along with Coulomb scattering of the stored beam during multiple traversals of the injection foil. Calculations and simulations of the losses are in reasonable agreement with measurements.

Introduction

The Proton Storage Ring (PSR) at Los Alamos functions as a high-current accumulator to provide intense pulses of 800 MeV protons for the Los Alamos Neutron Scattering Center (LANSCE) spallation neutron source. An 800 MeV  $\text{H}^-$  beam from the LAMPF linac is converted to  $\text{H}^0$  in a high-field stripper magnet; the  $\text{H}^0$  beam then enters the lattice through a dipole and is stripped to  $\text{H}^+$  beam with 92% efficiency in a  $200 \mu\text{g}/\text{cm}^2$  carbon foil. Up to 2800 turns are injected and accumulated in PSR during a single macropulse. Beam is normally extracted in a single turn shortly after the end of injection.

In the present operation at  $30 \mu\text{A}$ , slow losses of  $\sim 0.5 \mu\text{A}$  during accumulation have caused activation at the limit acceptable for hands-on-maintenance. These losses occur principally in the injection and extraction regions which contain the known limiting apertures. Further information on the design and initial performance are published elsewhere.<sup>1</sup>

General Characteristics of the Accumulation Losses

Slow losses are measured to  $\sim 30\%$  accuracy with a series of scintillator-based radiation detectors located on the outside wall of the tunnel at beam height opposite each ring dipole. Detector gains are all identical; signals from each as well as a sum signal of all detectors are used for loss measurements. The sum signal is calibrated by allowing a measured quantity of beam to be completely lost. Fast analog current signals, obtained directly from the phototubes, are available in the control room for detailed analysis of the time structure.

The sum current signal is a measure of the beam loss rate,  $\dot{L}(t)$ . A trace from normal operation is shown in Figure 1 along with a signal from a current monitor that senses the circulating beam current,  $I(t)$ . The ring current is a ramp because beam is continually injected during the injection period of  $375 \mu\text{s}$ . Figure 1 shows that  $\dot{L}$  is nearly proportional to the stored beam intensity. Total losses,  $L = \int \dot{L} dt$ , will then be quadratic in time. To increase the average current to  $100 \mu\text{A}$  we need to inject for  $\sim 1000 \mu\text{s}$ , but the losses under these conditions are an order of magnitude higher than for the present operation at  $375 \mu\text{s}$  which already produces the maximum acceptable activation of ring components.

Losses for an extended period of accumulation can arise from those occurring at the time of injection as well as from continual losses of the stored beam. The two components can be separated in an experiment where beam is accumulated for a short time ( $\sim 100 \mu\text{s}$ ) and stored for a much longer period ( $\sim 1000 \mu\text{s}$ ) before

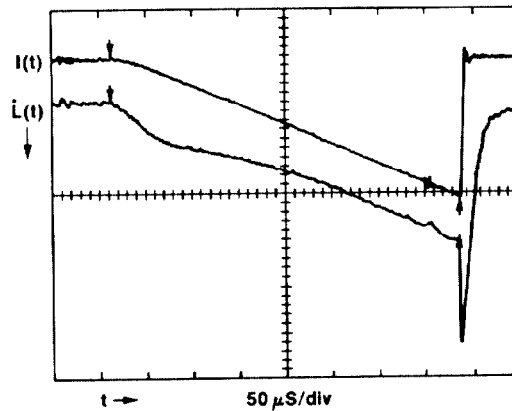


Figure 1. Loss Rate During Normal Operation

extraction. Loss rates and circulating current signals from one such experiment for a coasting beam (RF buncher off) are shown in Figure 2. The discontinuity at the end of injection is caused by the cessation of "first turn" or injection losses and amounts to  $\sim 2 \times 10^{-3}$  of the injected beam current. The loss rate during storage is a slowly increasing function of storage time with a fractional loss rate of  $\sim 1.3 \times 10^{-5}$  per proton per turn at the end of the  $100 \mu\text{s}$  injection period.

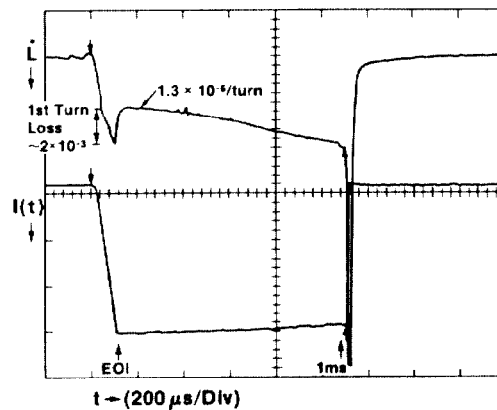


Figure 2. Loss Rate for 1 ms Storage

The significant loss observed during injection and the continual losses thereafter suggest that the injected beam somewhat more than fills the acceptance of PSR. This is corroborated by halo plate scans of the horizontal beam profile in the ring in which a thick plate is scanned across the ring aperture and the fraction of the beam intercepted by the plate is obtained by measuring the scattered beam intensity in the sum of several loss monitors. The signal is normalized to unity when all of the beam is intercepted. This technique is especially useful for measuring the beam distribution in the extremities of the beam. Data from one scan are shown in Figure 3 for the situation where beam is extracted shortly ( $10 \mu\text{s}$ ) after the end of  $100 \mu\text{s}$  of accumulation. The scan provides a good measure of the beam distribution just after capture in the ring and before foil scattering can cause appreciable emittance growth. In Figure 3 it is readily apparent that the beam distribution extends to about 38 mm which corresponds to the value of the limiting aperture defined by the extraction septum.

\* Work performed under the auspices of the United States Department of Energy.

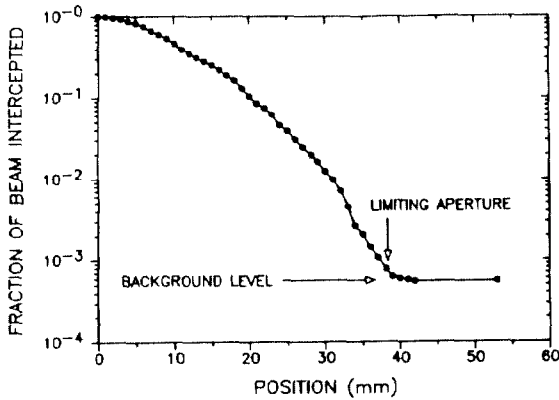


Figure 3. Horizontal Haloplate Scan

The beta functions at the septum and at the halo plate are nearly equal.

Emittance Growth and Losses During Injection

It may seem surprising that the beam fills the horizontal acceptance at injection since the acceptance of PSR,  $\sim 130\pi$  mm-mrad, is so much larger than the rms emittance,  $\sim 0.5\pi$  mm-mrad, of the  $H^-$  beam from LAMPF. The momentum spread (rms) of the  $H^-$  beam is also small with  $\Delta p/p \approx 5 \times 10^{-4}$ . Two main factors contribute to emittance growth in the injection process: 1) an increase in horizontal divergence in the stripper magnet when  $H^-$  is converted to  $H^0$  and 2) a large horizontal optics mismatch of the  $H^0$  beam to the PSR acceptance.

Stripping of the  $H^-$  in a high magnetic field is a stochastic process which leads to random fluctuations in the point of conversion and thus an increase in  $H^0$  beam divergence. Calculations of the angular distribution for a pencil beam of  $H^-$  are shown in Figure 4 for two different vertical entrance positions ( $y = 0$  at midplane and  $y = -4$  mm). The calculation used the measured field map of the stripper magnet and a parameterization of the  $H^-$  lifetime from earlier Los Alamos work.<sup>2</sup> Emittance growth in the stripper magnet is minimized by use of a small gap magnet with a high field gradient at the entrance and by optics which produce a very small waist in both  $x$  and  $y$  at the stripper magnet. Even with this optimization the horizontal emittance of the  $H^0$  is three (3) times larger than that of the incoming  $H^-$  beam.

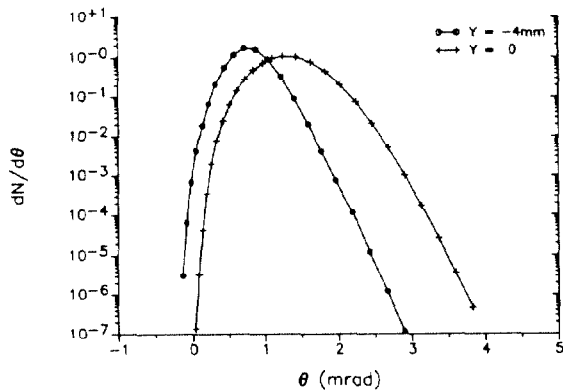


Figure 4.  $H^0$  Distribution After Stripper Magnet

An optics mismatch at injection is an additional consequence of magnetic stripping. The  $H^0$  is constrained to diverge from a small waist and cannot be matched simultaneously in the  $(X, X')$  and  $(Y, Y')$  planes. At the standard location of the foil stripper, the  $H^0$  is reasonably well matched in  $(Y, Y')$  but badly mismatched in the  $(X, X')$  plane. The mismatch factor,  $C = \{\beta_o \gamma_R + \beta_R \gamma_o - 2\alpha_o \alpha_R\}/2$ , (subscript  $o$  refers to  $H^0$  and

$R$  to the ring) has a value of 3.5 indicating a further increase of 3.5 in the rms emittance of the stored beam. The mismatch also changes the beam distribution; for a Gaussian beam injected on axis, one can easily obtain the following closed form for the distribution of the invariant betatron amplitude,  $y$ :

$$P(y)dy = \frac{1}{\epsilon_o} e^{-\frac{Cy^2}{2\epsilon_o}} I_o \left( \frac{y^2}{2\epsilon_o} \sqrt{C^2 - 1} \right) y dy \quad (1)$$

where  $\epsilon_o$  is the rms emittance of the incoming  $H^0$  beam and  $I_o$  is a modified Bessel Function.<sup>3</sup> The rms emittance for this distribution is  $C\epsilon_o$ . This distribution has longer "tails" than a Gaussian with the same rms emittance thereby increasing still further the size of the beam near the limiting apertures. The non-gaussian tails are readily apparent at PSR in wire scanner profiles of the extracted beam taken at the end of short ( $100 \mu s$ ) accumulation as shown in Figure 5. The "mismatched" Gaussian distribution derived from equation (1) fits the data very well whereas a Gaussian with the same rms width fits poorly; especially at large  $X$ .

Integration of the distribution described by equation (1) for the region outside of the limiting aperture provides an estimate of injection or "first turn" losses. A value of 2 to  $4 \times 10^{-3}$  is obtained which is in good agreement with the observed value of  $\sim 2 \times 10^{-3}$  considering the high sensitivity of the result to the size of the limiting aperture.

EXTRACTION WIRE SCANNER PROFILE  
(INITIAL BEAM DISTRIBUTION)

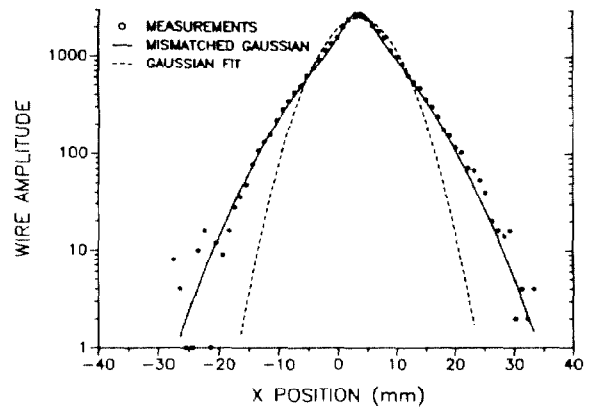


Figure 5. Extraction Wire Scanner Profile

Emittance Growth and Losses During Storage

A typical proton in PSR traverses the injection foil during about half of its revolutions. Multiple Coulomb scattering in the foil will cause emittance growth (rms) given by  $\epsilon(t) = \epsilon_o + \beta_f \theta_1^2 f N(t)/2$  where  $\epsilon_o$  is the initial rms emittance,  $\beta_f$  the beta function at the foil,  $\theta_1$  the rms scattering angle from a single foil traversal and  $fN(t)$  the number of foil traversals in  $N$  turns up to time  $t$ . The rms emittance is defined as  $\sqrt{\langle X^2 \rangle \langle \theta^2 \rangle - \langle X\theta \rangle^2}$  where  $\langle \rangle$  indicates expectation value and  $\theta = X'$ . Measurements of beam sizes as a function of storage time are well fit by the above equation for  $\epsilon(t)$  and show nearly a factor of 3 increase of emittance during 1 ms of storage.

To estimate accurately losses from multiple Coulomb scattering requires more than knowledge of the rms emittance growth; one must calculate the evolution of the distribution function with time. We have made estimates using two different methods which produce similar results in reasonable agreement with measurements. The first method used a Fokker-Planck equation which was derived for estimating beam life-

$$\frac{1}{K} \frac{\partial P}{\partial t}(t, y) = \frac{\partial}{\partial y} \left[ y \frac{\partial}{\partial y} \left( \frac{P(y)}{y} \right) \right] \quad (2)$$

times in the presence of Coulomb scattering by residual gases.<sup>4</sup> Here  $y$  is the invariant betatron ampli-

tude and  $K$  a constant. Solutions for the distribution function,  $P$ , are obtained as a Fourier-Bessel series and integrated to obtain the losses.

Similar results are obtained with the Monte Carlo tracking code, ARCHSIM, developed by one of the authors for modeling circular machines. The tracking code simulates emittance growth in the stripper magnet and treats scattering in the stripper foil as a combination of multiple Coulomb scattering with single Coulomb and nuclear tails. Results from the simulation and from solutions of the Fokker-Planck equation made using measured values of parameters in the models are compared in Figure 6 with measured data on loss rates. Agreement between calculations and measurements are within the calibration uncertainties of the losses and the errors on parameters in the calculations. Losses are sensitive to several parameters including the mismatch factor and  $H^0$  distribution, but especially, to the size of the limiting aperture. With small adjustments of parameters, within errors, both calculations can be made to agree completely with the loss rate data.

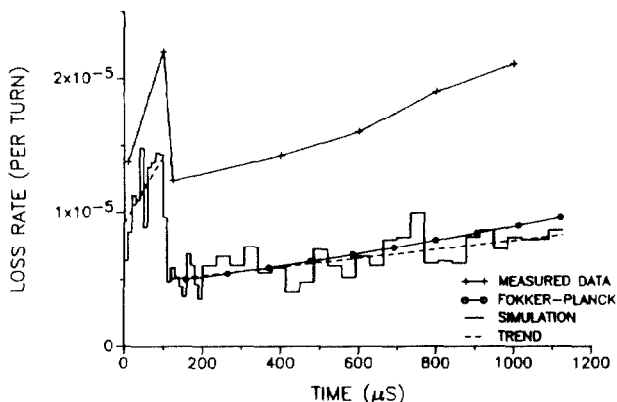


Figure 6. Loss Rate Calculations and Measurements  
Effect of the RF Buncher

An RF buncher is used to maintain an empty gap to accommodate the extraction kicker rise time. Synchrotron motion induced by the buncher increases the momentum spread to  $\sim 0.3\%$ ; because of dispersion the beam size increases by several mm and also contributes to beam losses. For long storage, this shows up as a

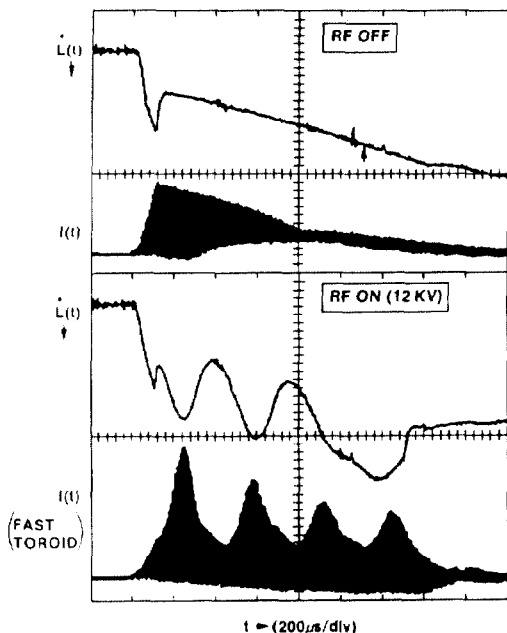


Figure 7. Effect of RF Buncher on Loss Rate

striking modulation of the loss rate with a frequency twice that of the synchrotron oscillations as shown in Figure 7. Losses are increased by about 45% when the RF is on at typical operating set points.

Other Contributions

Losses from nuclear scattering are readily estimated from the total cross section as  $3.3 \times 10^{-6}$  per foil traversal. The contribution from large angle single Coulomb scattering is often overlooked. Because the cross section falls off only as a power law rather than as an exponential it contributes a long tail to any beam distribution. This was seen at PSR when the injection foil location was changed to provide a better match in the  $(X, X')$  plane. The halo plate scan of the beam distribution (after a short accumulation) plotted in Figure 8 shows the expected reduction in size of the core of the beam. Also seen is a tail extending to the limiting aperture. The size and shape of the tail agrees with analytical and Monte Carlo calculations of the contribution from single Coulomb scattering. At PSR large-angle Coulomb scattering contributes a loss rate of  $1.5 \times 10^{-6}$  per foil traversal for a  $\delta$  function initial distribution and more for a beam of finite emittance.

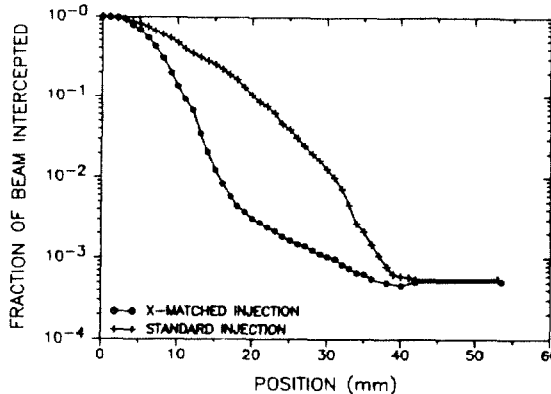


Figure 8. Evidence for Single Coulomb Scattering

Summary

The composition of accumulation losses during standard operation of PSR (375  $\mu$ s injection period) can be determined from the data and analysis presented here. Results are listed below:

"First Turn"	0.20%
Nuclear and Large-Angle Coulomb Scattering	0.15%
Emittance Growth in Absence of RF	0.70%
Effect of RF	<u>0.50%</u>
Total	1.55%

References

- [1] G. Lawrence, "The Performance of the Los Alamos Proton Storage Ring," Proc 1987 IEEE Particle Accelerator Conference, pp. 825-829.
- [2] A. Jason, D. Hudgins, and O. van Dyck, "Neutralization of H- Beams by Magnetic Stripping," IEEE Trans. Nucl. Sci., NS-28, pp. 2704-2706 (1981).
- [3] R. Macek, "PSR Beam Distributions II: Mismatched Gaussian," Los Alamos National Laboratory PSR Technical Note #153, October 1987.
- [4] H. Bruck, "Circular Particle Accelerators," LA-TR-72-10 Rev., Chap XIV (1972). Translation from French original "Accélérateur Circulaires de Particules" (1966).